Supplemental Information

Light absorption and scattering properties of indole secondary organic aerosol prepared under various oxidant and relative humidity conditions

Vahe J. Baboomian,[a] Quanfu He,[b] Julia Montoya-Aguilera,[a] Nabila Ali,[a] Lauren T. Fleming,[a] Peng Lin,[c] Alexander Laskin,[c] Julia Laskin,[c] Yinon Rudich,[b*] and Sergey A. Nizkorodov[a*]

[a] Department of Chemistry, University of California, Irvine, California 92697, USA

[b] Department of Earth and Planetary Sciences, Weizmann Institute of Science, Rehovot 76100, Israel

[c] Department of Chemistry, Purdue University, West Lafayette, Indiana 47907, USA

* Corresponding author e-mails: yinon.rudich@weizmann.ac.il and nizkorod@uci.edu

Section S1. Testing the effect of starting indole concentration in the chamber on MAC

HPLC-PDA-HRMS (see Table S2 below) analysis showed that dimers contribute significantly to the pool of chromophoric compounds in indole-derived SOA. Oligomer formation may be affected by SOA precursor concentrations with higher concentrations favoring oligomer formation (that would be less likely under much lower ambient concentration conditions). Therefore, indole+NO$_3$ SOA was prepared under different indole mixing ratios to explore the effect on the absorption coefficient of SOA samples. As shown in Figure S1, the indole+NO$_3$ SOA mass absorption coefficient did not significantly depend on the starting indole mixing ratios (50-200 ppb) explored in this study, therefore 200 ppb of indole was used in most of the experiments reported here in order to collect sufficient SOA mass for offline analysis. The lack of sensitivity of the spectra to the indole concentration suggests that the dimers (responsible for the 600 nm band) are produced by particle-phase chemistry as opposed to gas-phase chemistry.
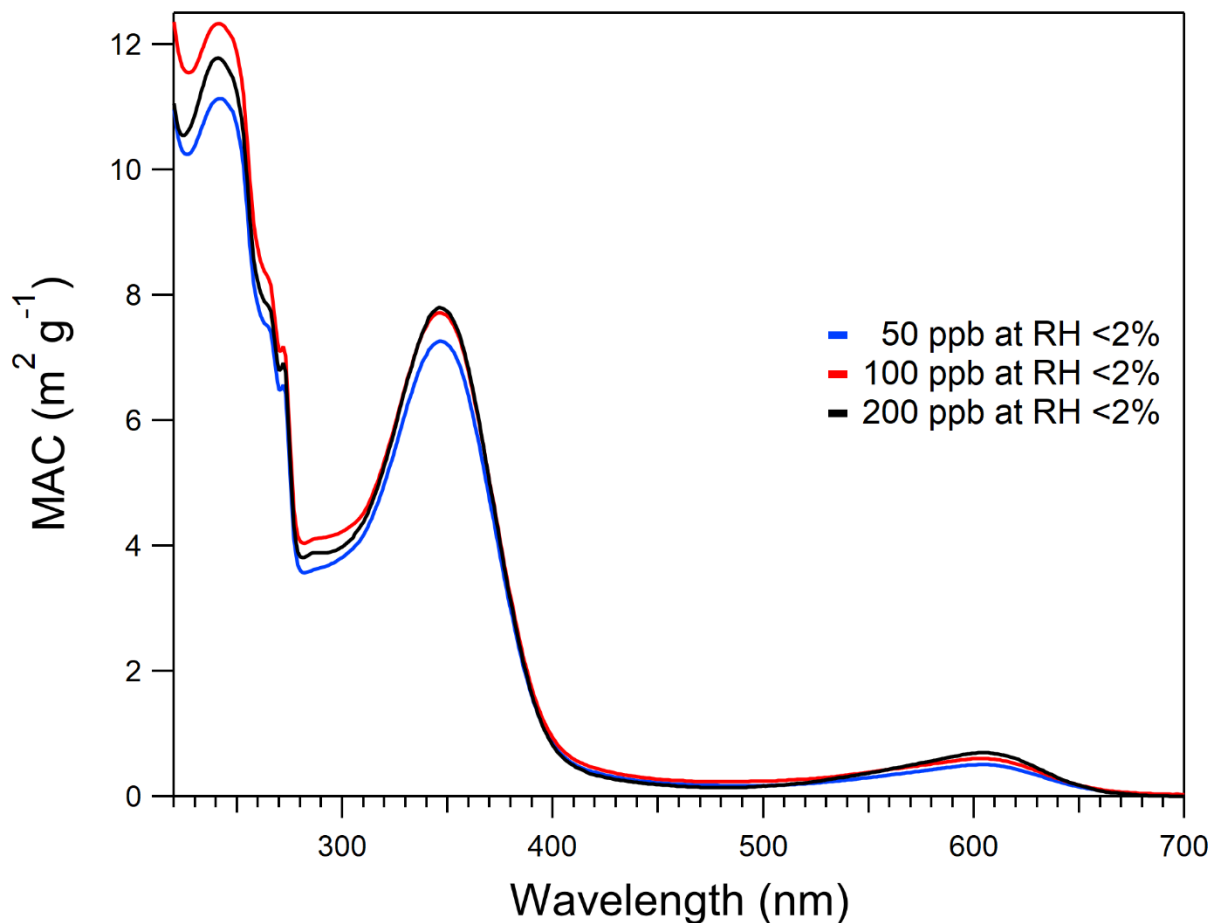
Figure S1. Wavelength-dependent *MAC* of indole + NO$_3$ SOA for different starting mixing ratios of indole.

Section S2. Testing the completeness of extraction of light-absorbing compounds

Figure S2 shows Teflon filters with indole+OH SOA (left), indole+O$_3$ SOA (middle), and indole+NO$_3$ SOA (right) particles generated under dry condition (<2% RH). The intensity and hue of the color varied between samples of the same SOA type collected on different days due to the varying amount of SOA collected (0.5-2.5 mg).
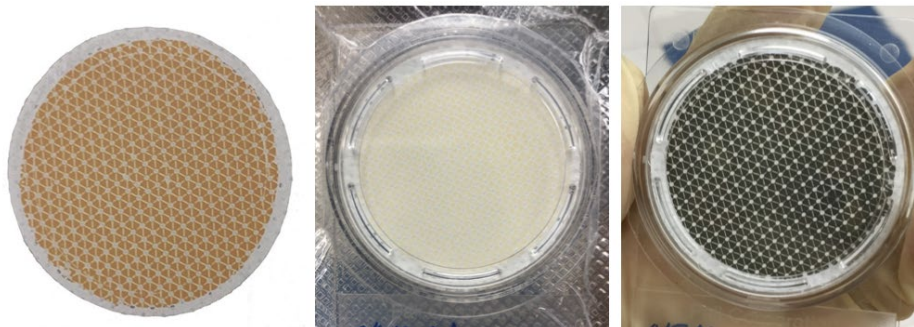
Figure S2. Sample photographs of filters containing indole+OH SOA (left), indole+O$_3$ SOA (middle), and indole+NO$_3$ SOA (right) particles.

Upon the first extraction, the filters changed from colored to white suggesting most of the chromophores were extracted. To check whether any soluble material remains on the filter, multiple extractions from the same filter were performed. Each extraction consisted of placing the filter in 5 mL of methanol and placing the solution on a shaker for 5 minutes. The filter was allowed to dry between extractions. The solution obtained from the first extraction saturated the detector. Therefore, the solution was diluted by a factor of 10, and the absorbance values were multiplied by 10 to generate the dotted trace in Fig. S3. Across the UV-Vis spectrum, the absorbance of extraction 1 was 20-30 times higher than that of extraction 2, suggesting that the first extraction extracted >95% of the soluble material. Note that indole oxidation products should have strong $\pi\rightarrow\pi^*$ bands in the UV. In combination with the white color of the filter following the extraction, we believe that all the major constituents of indole SOA are fully soluble in methanol at the solution concentrations level (typically 0.1-0.5 μg/mL) used in this work.
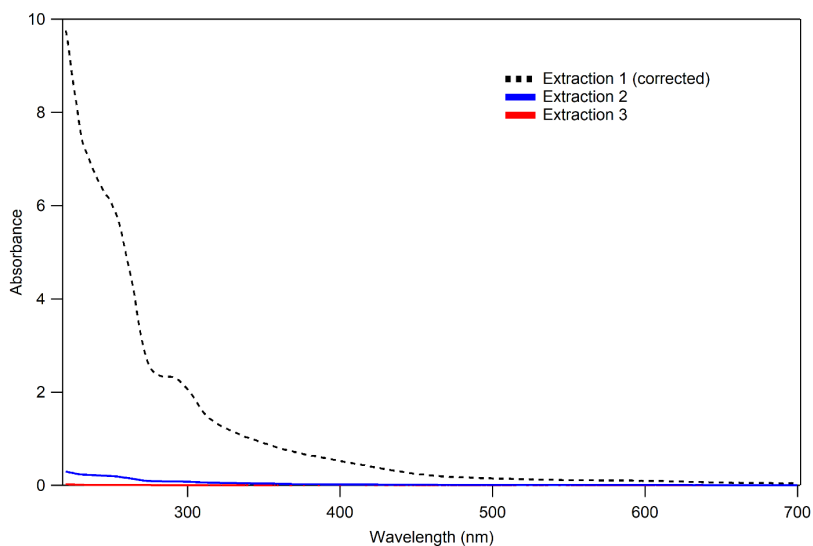
Figure S3. UV-Vis absorption spectra for sample of indole + O$_3$ SOA at 25% RH extracted multiple times.

Section 3. Densities and elemental ratios of SOA particles produced in the oxidation flow reactor

Table S1. Effective densities and elemental ratios of SOA particles produced in OFR experiments. The standard deviations (STD) correspond to one sigma for the density.

Oxidants	RH	N_2O	Effective Density g/cm^3	STD g/cm^3	H/C	O/C	N/C
OH	38.2	0	1.33	0.02	1.080	0.970	0.104
	37.1	1%	1.15	0.01	1.075	1.039	0.109
	37.6	2%	1.17	0.01	1.048	0.791	0.125
	37.6	4%	1.31	0.01	0.937	0.699	0.130
NO$_3$	<2%	0%	1.29	0.01	1.060	0.777	0.114
	25%	0%	1.13	0.05	0.893	0.460	0.115
	51%	0%	1.24	0.03	0.895	0.520	0.119
	76%	0%	1.18	0.06	0.916	0.588	0.117
O$_3$	<2%	0%	1.05	0.03	1.062	0.780	0.112

Section 4. Absorption Ångström Exponent (AAE)

The *MAC* values of the chamber generated SOA can be used to calculate the Absorption Ångström Exponent (*AAE*), an empirical parameter used to describe the wavelength dependence of *MAC*:

$$MAC\ (\lambda) = MAC_0 \times \lambda^{-AAE} \tag{1}$$

Since *k* is proportional to the product of *MAC* and wavelength

$$k\ (\lambda) = \frac{MAC\ (\lambda) \times \rho \times \lambda}{4\pi} \tag{2}$$

The analogous equation for *k* would take the form

$$k\ (\lambda) = k_0 \times \lambda^{-w} \tag{3}$$

Where *w* = *AAE*-1, as defined by Saleh (2020). The *w* values were obtained by fitting the dependence of the *k* values to base-10 logarithm of wavelength (in nm) to a linear function:

$$log[k\ (\lambda)] = const - w \times log[\lambda] \tag{2}$$

The fit was constrained to 250-630 nm range because *MAC* values above 630 nm were too close to the detection limit. The results, along with the fitted *w* values, are shown in in Figure S4. Figure S5 shows the resulting *w* values and *k* values at 550 nm based on the classification of BrC by Saleh (2020).

Saleh (2020) *From Measurements to Models: Toward Accurate Representation of Brown Carbon in Climate Calculations*. Current Pollution Reports 2020, 6 (2), 90-104. DOI:10.1007/s40726-020-00139-3.
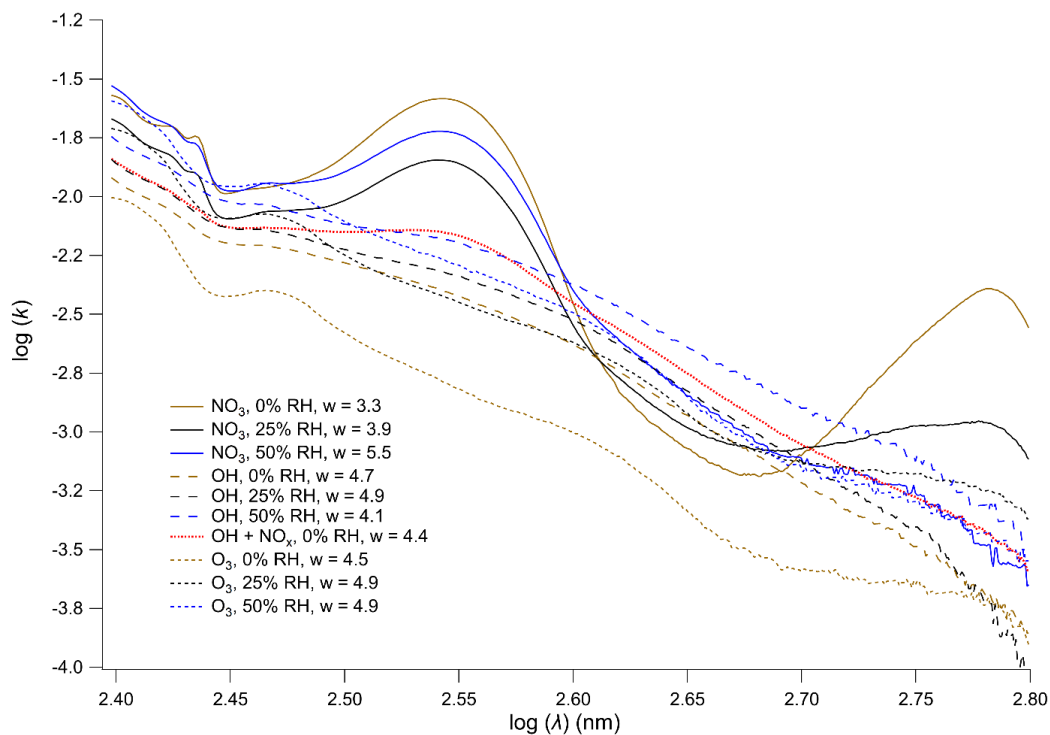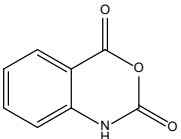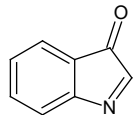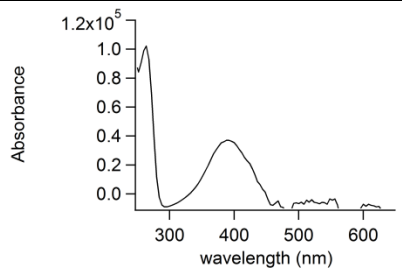
Figure S4. Log-Log plot of k as a function of wavelength for chamber-generated SOA. The effective AAE values obtained from linear fits of these spectra in the 250-630 nm range are given in the legend (the trendlines are not shown to avoid clutter in the figure).
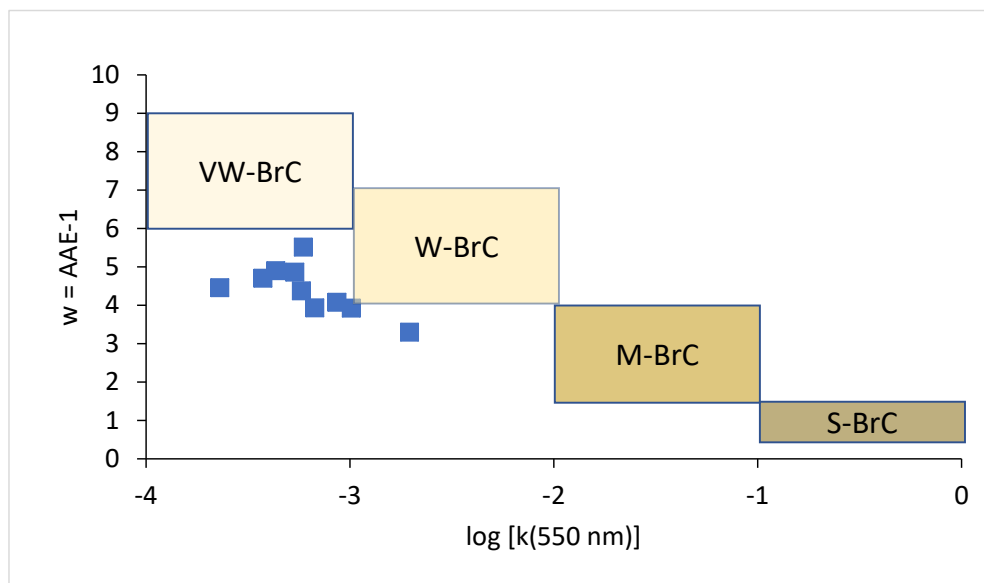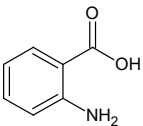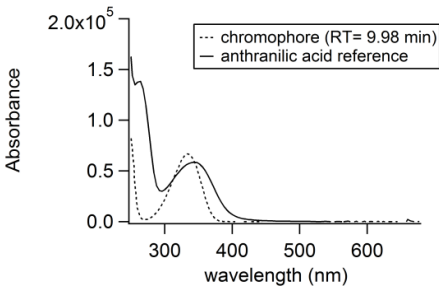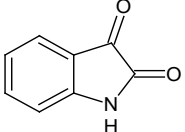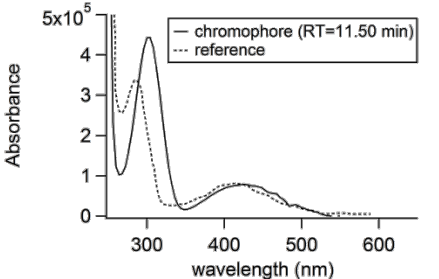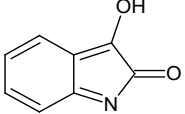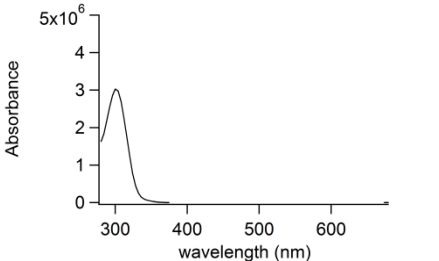

Figure S5. Values of w and log[k(550 nm)] (filled squares) for the chamber-generated SOA on the Saleh (2020) BrC classification plot.
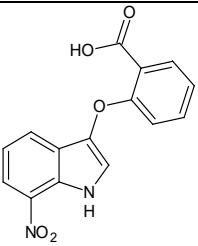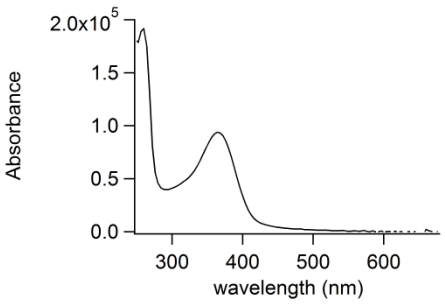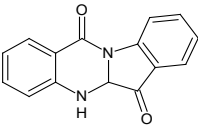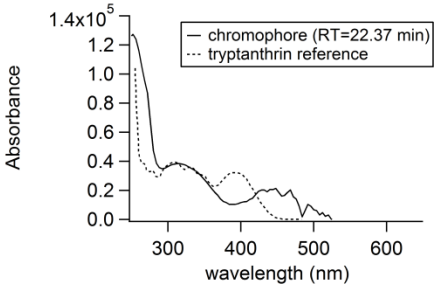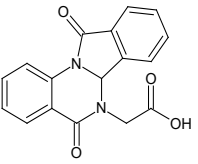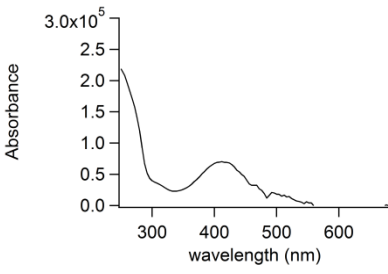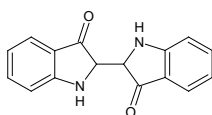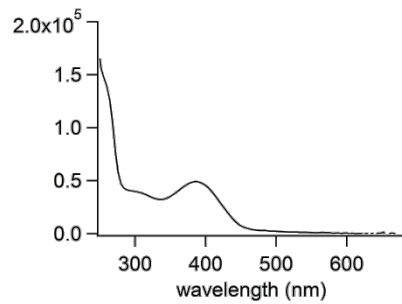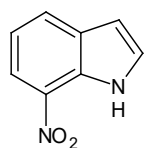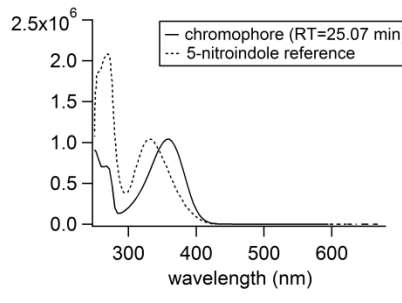
Section 5. Tentative assignments of chromophores
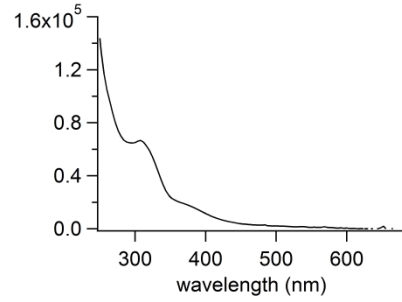
Table S2. Possible chromophores from indole + NO_3 SOA, indole + O_3 SOA, and indole + OH SOA generated at low relative humidity (<2% RH). Data were acquired by using the HRMS setup with column A, and the retention times correspond to column A. The HRMS data for the indole+OH +NOx SOA were not recorded, so they are not included in this table. For some compounds, multiple retention times are listed because multiple isomers with the same formula are observed. Note that the measured and reference absorption spectra do not exactly match because of co-elution of various species. The compounds were observed as protonated ions (monoisotopic *m/z* values are provided in the 2nd column).
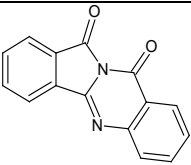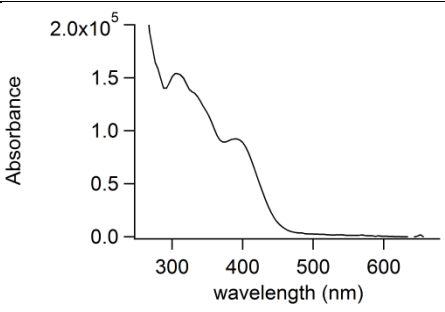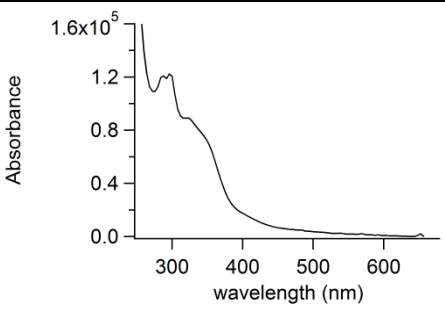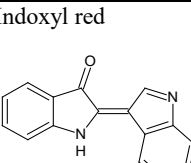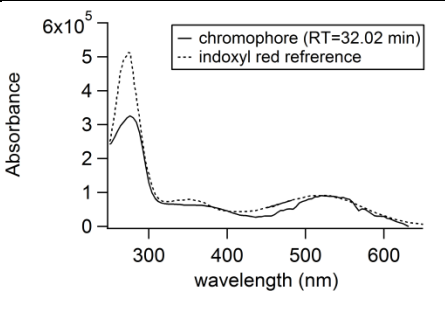
Retention time on column A (min)	Theoretical *m/z* of the protonated ion	Elemental formula of the neutral	Tentative assignment	UV-Vis Absorption spectrum	Indole + NO₃ SOA	Indole + O₃ SOA	Indole + OH SOA
4.54	164.0342	$C_8H_5NO_3$	Isatoic anhydride				X
7.69 (NO₃) 8.4 (O₃)	132.0444	C_8H_5NO	Oxyindole		X	X	
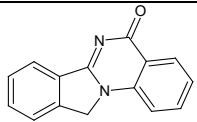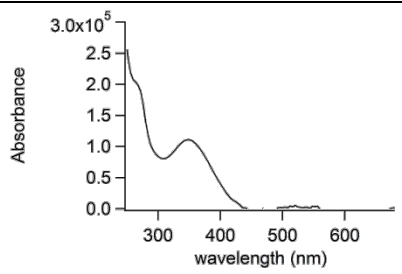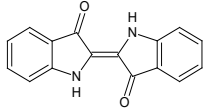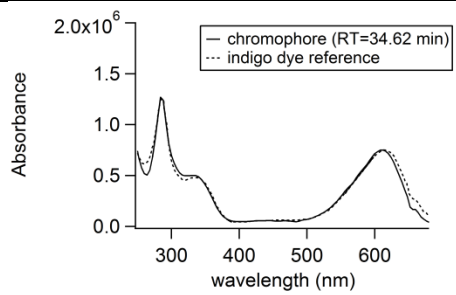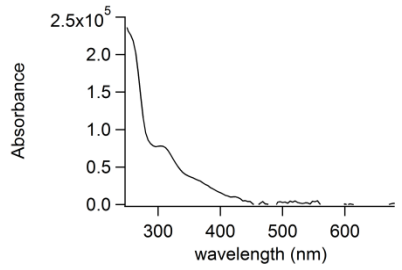
9.98	138.0550	$C_7H_7NO_2$	Anthranilic acid			X	
11.5 (NO$_3$) 12.31 (O$_3$)	148.0393	$C_8H_5NO_2$	Isatin		X	X	
14.82 (NO$_3$) 15.55 (O$_3$)	148.0393	$C_8H_5NO_2$			X	X	
18.37	299.1026	$C_{16}H_{14}N_2O_4$					X
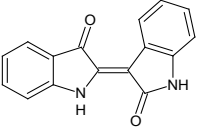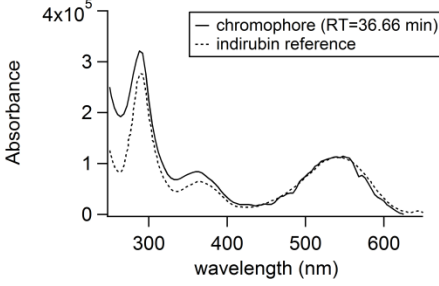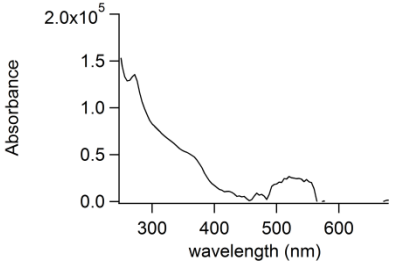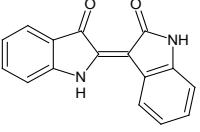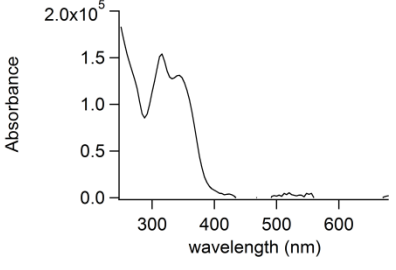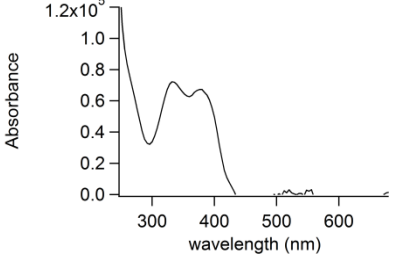
18.61	299.0662	$C_{15}H_{10}N_2O_5$				X	
20.94	283.1077	$C_{16}H_{14}N_2O_3$					X
22.37 (NO$_3$) 22.66 (O$_3$) 36.54 (OH)	251.0815	$C_{15}H_{10}N_2O_2$	Tryptanthrin 		X	X	X
23.69	309.0870	$C_{17}H_{12}N_2O_4$			X		
23.76	253.0972	$C_{15}H_{12}N_2O_2$					X

RT	m/z	Formula	Name	Spectrum			
24.09 (O_3) 23.03 (OH)	265.0972	$C_{16}H_{12}N_2O_2$	Dihydro indigo dye			X	X
25.07	163.0502	$C_8H_6N_2O_2$	Nitroindole		X		
28.02	285.0870	$C_{15}H_{12}N_2O_4$				X	
28.39	233.0709	$C_{15}H_8N_2O$					X

30.58 (NO₃) 30.81 (O₃)	249.0659	$C_{15}H_8N_2O_2$			X	X	
31.17	283.0713	$C_{15}H_{10}N_2O_4$				X	
32.02 (NO₃) 43.03 (OH)	247.0866	$C_{16}H_{10}N_2O$	Indoxyl red 		X		X
32.18	297.0870	$C_{16}H_{12}N_2O_4$					X

RT	Mass	Formula	Structure	UV spectrum			
32.68	235.0866	$C_{15}H_{10}N_2O$			X		
32.99	428.1241	$C_{24}H_{17}N_3O_5$					X
34.62 (NO₃) 34.77 (O₃) 41.18 (OH)	263.0815	$C_{16}H_{10}N_2O_2$	Indigo dye 		X	X	X
35.63	325.0931	$C_{16}H_{12}N_4O_4$			X		
36.57	249.1022	$C_{16}H_{12}N_2O$					X

36.66 (NO$_3$) 36.84 (O$_3$) 42.81 (OH)	263.0815	C$_{16}$H$_{10}$N$_2$O$_2$	Indirubin		X	X	X
37.55	392.1030	C$_{24}$H$_{13}$N$_3$O$_3$			X		
38.3 (NO$_3$) 38.45 (O$_3$)	263.0815	C$_{16}$H$_{10}$N$_2$O$_2$	Isoindigo or Isoindirubin		X	X	
40.75	279.0877	C$_{15}$H$_{10}$N$_4$O$_2$			X		

Section 6. Time-of-Flight Aerosol Mass Spectrometer results

Based on AMS data, chemical families that showed a similar RH dependence to the measured k values were the C_xH_yO and $C_xH_yO_z$ families (Fig. S6). On the other hand, families like NO^+ and $C_xH_y^+$ followed the opposite RH dependence as the k values. While we do not have an explanation for this trend, the data suggest that at least two competing mechanisms operate, with one favoring dry conditions (<2% RH), and the other favoring humidified conditions.
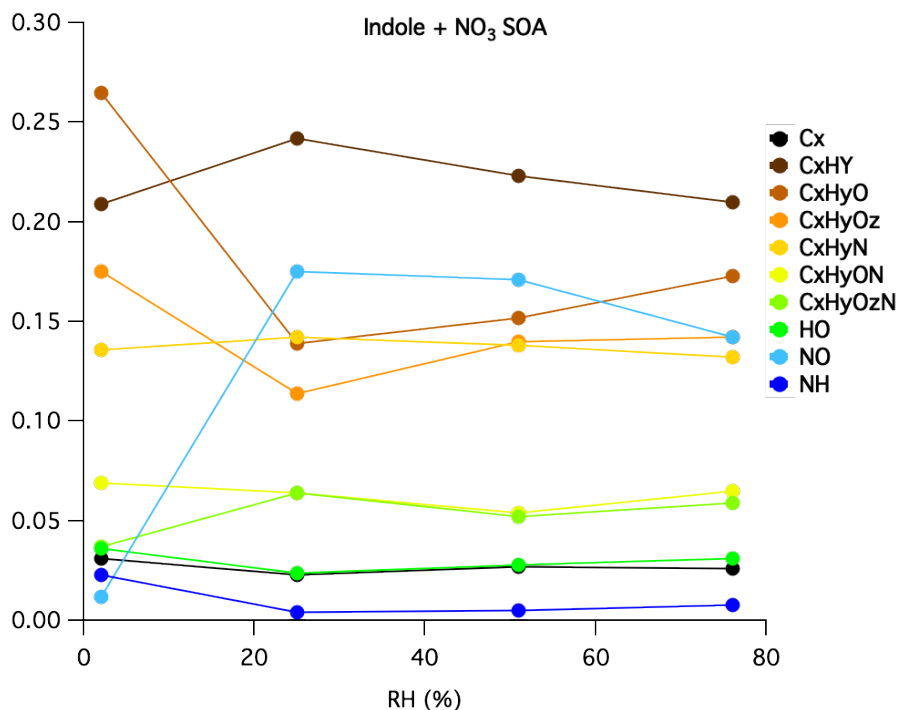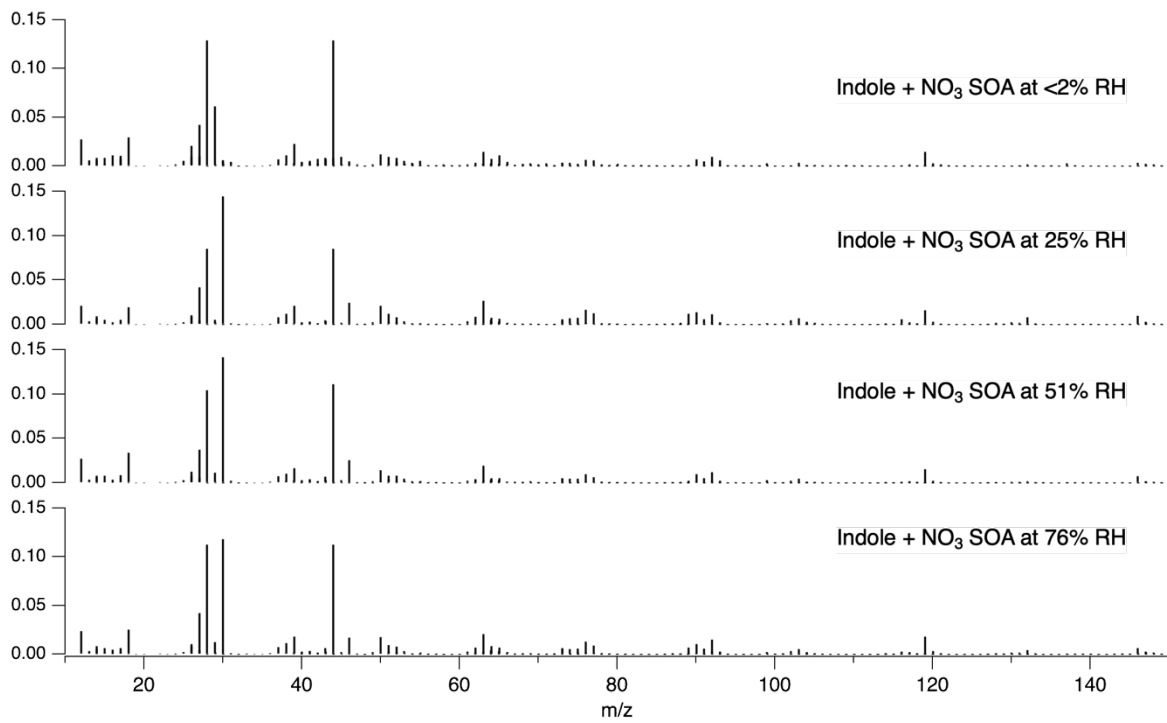

Figure S6. Indole + NO$_3$ SOA: AMS Families vs RH

Figure S7. Sample ToF-AMS mass spectra of indole + NO₃ SOA preparaed in the OFR.